MOBODY: MODEL-BASED OFF-DYNAMICS OFFLINE REINFORCEMENT LEARNING

Anonymous authors
Paper under double-blind review

ABSTRACT

We study off-dynamics offline reinforcement learning, where the goal is to learn a policy from offline source and limited target datasets with mismatched dynamics. Existing methods either penalize the reward or discard source transitions occurring in parts of the transition space with high dynamics shift. As a result, they optimize the policy using data from low-shift regions, limiting exploration of high-reward states in the target domain that do not fall within these regions. Consequently, such methods often fail when the dynamics shift is significant or the optimal trajectories lie outside the low-shift regions. To overcome this limitation, we propose MOBODY, a Model-Based Off-Dynamics Offline RL algorithm that optimizes a policy using learned target dynamics transitions to explore the target domain, rather than only being trained with the low dynamics-shift transitions. For the dynamics learning, built on the observation that achieving the same next state requires taking different actions in different domains, MOBODY employs separate action encoders for each domain to encode different actions to the shared latent space while sharing a unified representation of states and a common transition function. We further introduce a target Q-weighted behavior cloning loss in policy optimization to avoid out-of-distribution actions, which push the policy toward actions with high target-domain Q-values, rather than high source domain Q-values or uniformly imitating all actions in the offline dataset. We evaluate MOBODY on a wide range of MuJoCo and Adroit benchmarks, demonstrating that it outperforms state-of-the-art off-dynamics RL baselines as well as policy learning methods based on different dynamics learning baselines, with especially pronounced improvements in challenging scenarios where existing methods struggle.

1 INTRODUCTION

Reinforcement learning (RL) (Kaelbling et al., 1996; Li, 2017) aims to learn a policy that maximizes cumulative reward by interacting with an environment and collecting the corresponding rewards. While RL has led to impressive successes in many domains, such as autonomous driving (Kiran et al., 2021) and healthcare (Lee et al., 2023), it faces significant constraints on interaction with the environment due to safety or cost concerns. One solution is to learn a policy from a pre-collected offline dataset (Levine et al., 2020). Still, when the offline dataset is insufficient, data from another environment, such as a simulator with potentially mismatched dynamics, may be needed, but requires further domain adaptation. In our paper, we study a specific type of domain adaptation in RL, called off-dynamics offline RL (Liu et al., 2022; 2024; Lyu et al., 2024b), where the simulator (source) and real/deployed (target) environments differ in their transitions. The agent is not allowed to interact with the environment but only has access to offline data that is pre-collected from the two domains with mismatched dynamics and trains a policy with the offline data.

Existing works on off-dynamics offline RL solve the problem by 1) reward regularization methods (Liu et al., 2022; 2024; Wang et al., 2024) or 2) data filtering methods (Xu et al., 2023; Wen et al., 2024) that penalize or filter out source transitions with high dynamics shift. As a result, the policy is mostly optimized with the transitions from the low shift regions, limiting exploration of high-reward states in the target domain that do not fall within these regions. Consequently, such methods often fail when the dynamics shift is significant or the optimal/high-reward trajectories lie outside the low-shift regions. So we wonder, can we directly optimize the policy with the target transition, instead of only the low-shift regions to allow for more exploration of the high target reward and large shift region?

Motivated by this, we propose a Model-Based Off-Dynamics RL algorithm (MOBODY) that learns target domain dynamics through representation learning and optimizes the policy with *exploratory* rollout from the learned dynamics instead of only the low-shift region data. Existing dynamics learning methods, such as learning with limited target data, learning with combined source and target data, and pretraining on source and finetuning on the target domain, are infeasible in the off-dynamics RL setting due to the intrinsic dynamics difference in this problem. This is because 1) the dynamics learned from the combined dataset is not the accurate target dynamics, but the dynamics resemble the source one as the source transitions dominate the dataset, 2) the pretrain-finetune method still doesn't capture what is the difference between source and target dynamics using the same dynamics model, but only tries to learn the target domain based on the source transition.

To learn the target dynamics, we leverage shared structural knowledge across domains, such as the high-level robot motion and position in a robotics task, while employing separate modules to account for domain-specific dynamics differences. Specifically, we observe that to achieve the same next state starting from the same state, different actions are required in two domains. Based on this, we propose to learn separate action encoders for the two dynamics to encode actions into a unified action representation, and also learn a unified transition and state encoder to map the unified latent state and action representation to the next state. And such shared representation and transition functions can be learned with the auxiliary of the source data through representation learning. In this way, MOBODY learns separate transition functions for two domains but utilizes the source data to provide shared structure knowledge regarding the transitions. As shown in Figure 1, MOPO that directly learns dynamics with combined source and target data significantly underperforms MOBODY, which is specifically optimized to learn the *target* dynamics.

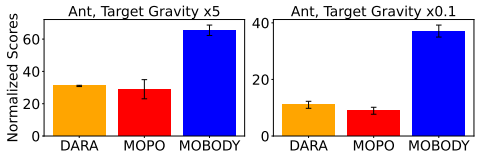

Figure 1: Comparison between DARA (Liu et al., 2022) (a SOTA model-free reward regularization method for offline off-dynamics RL), MOPO (Yu et al., 2020) (a vanilla model-based offline RL), and MOBODY on two MuJoCo tasks. We show that 1) the model-free method DARA receives low reward compared with model-based MOBODY due to a lack of exploration in the target domain, and 2) MOPO fails as it cannot learn a good transition for exploration with a combined source and target dataset.

We further propose a practical and useful target Q-weighted behavior cloning regularization in the policy learning to avoid out-of-distribution and high source Q value (but low target Q value) actions, inspired by the advantage-weighted regression (Peters & Schaal, 2007; Kostrikov et al., 2021a). The vanilla behavior cloning loss (Fujimoto & Gu, 2021) will push the policy to favor the action in the source data, but the action in the source data might not perform well in the target domain due to the dynamics shift. To overcome this issue, the target Q-weight behavior cloning loss regularization will up-weight action with the high *target* Q value.

Our contribution can be summarized as follows:

- We propose a novel paradigm for off-dynamics offline RL, called model-based off-dynamics offline RL, that can explore the target domain with the learned target transitions instead of optimizing the policy only with the low-shift transitions.
- We propose a novel framework for learning the *target* dynamics with source data and limited target data by learning separate action encoders for the two domains while also learning a shared state and the transition in the latent space. We also incorporate a Q-weighted behavior cloning loss for policy optimization that is simple, efficient, and more suitable for off-dynamics offline RL settings than vanilla behavior cloning loss.
- We evaluate our method on MuJoCo and Adroit environments in the offline setting with different types and levels of off-dynamics shifts and demonstrate the superiority of our model with an average 58% improvement over baseline methods on the gravity and friction settings and 25% on the kinematic and morphology shift settings.

2 Background

Off-dynamics offline reinforcement learning. We consider two Markov Decision Processes (MDPs): the source domain $\mathcal{M}_{\text{src}} = (\mathcal{S}, \mathcal{A}, R, p_{\text{src}}, \gamma)$ and the target domain $\mathcal{M}_{\text{trg}} = (\mathcal{S}, \mathcal{A}, R, p_{\text{trg}}, \gamma)$. The

difference between the two domains lies in the transition dynamics p, i.e., $p_{\text{src}} \neq p_{\text{trg}}$ or more specifically, $p_{\text{src}}(s' \mid s, a) \neq p_{\text{trg}}(s' \mid s, a)$. Following existing literature on off-dynamics RL (Eysenbach et al., 2020; Liu et al., 2022; Lyu et al., 2024a; Guo et al., 2024; Lyu et al., 2024b; Wen et al., 2024), we assume that reward functions are the same across the domains, which is modeled by the state, action, and next state, i.e., $r_{\text{src}}(s, a, s') = r_{\text{trg}}(s, a, s')$. The dependency of the reward on s' is well-justified in many simulation environments and applications, such as the Ant environment in MuJoCo, where the reward is based on how far the Ant moves forward, measured by the change in its x-coordinate (i.e., the difference between the x-coordinate after and before taking action). The goal is to learn a policy π with source domain data $(s, a, s', r)_{\text{src}}$ and limited target domain data $(s, a, s', r)_{\text{trg}}$ that maximize the cumulative reward in the target domain $\max_\pi \mathbb{E}_{\pi, p_{\text{trg}}}[\sum_t \gamma^t r_{\text{trg}}(s_t, a_t)]$. In the offline setting, we are provided with static datasets from a source and a target domain $\mathcal{D}_{\text{src}} = \{(s, a, s', r)_{\text{src}}\}$ and $\mathcal{D}_{\text{trg}} = \{(s, a, s', r)_{\text{trg}}\}$, which consist of the transitions/trajectories collected by some unknown behavior policy. Note that in the off-dynamics setting, the number of transitions from the target domain is significantly smaller than the source, i.e., $|D_{\text{trg}}| \ll |D_{\text{src}}|$, and normally the ratio $\frac{|D_{\text{src}}|}{|D_{\text{trg}}|}$ can vary from 10 to 200. In our paper, we follow the ODRL benchmark (Lyu et al., 2024b) in which the ratio is 200.

Model-based offline reinforcement learning. Model-based RL learns a transition function $\hat{T}(s', r|s, a)$ by maximizing the the likelihood $\hat{T} = \max_T \mathbb{E}_{D_{\text{offline}}}[\log \hat{T}(s', r|s, a)]$. Then, the algorithm rolls out new transition data to optimize the policy and take $u(s, a)$ as the uncertainty quantification to obtain a conservative transition, i.e., $(s, a, s', \hat{r} - \alpha u(s, a))$. The policy with offline data $\mathcal{D}_{\text{offline}}$ and online rollout $(s, a, s', \hat{r} - \alpha u(s, a))$. However, different from traditional model-based offline RL, we only have very limited target domain data and source data with dynamics shift. There is no existing model-based solution for off-dynamics RL, which calls for novel methodology development both in dynamics learning and policy learning.

Detailed discussions of related work are in Appendix A due to space limit.

3 MOBODY: Model-Based Off-Dynamics Offline Reinforcement Learning

In this section, we present our algorithm, MOBODY, for the off-dynamics offline RL problem setting. We first present how we learn the *target* dynamics with very limited target domain data $\mathcal{D}_{\text{trg}}$ and source domain data $\mathcal{D}_{\text{src}}$. Secondly, for policy learning, we incorporate a target Q-weighted behavior cloning loss to regularize the policy, where the target Q value is learned from *enhanced target data*, including reward regularized source data, target data, and rollout data from learned dynamics. The algorithm is summarized in Algorithm 2.

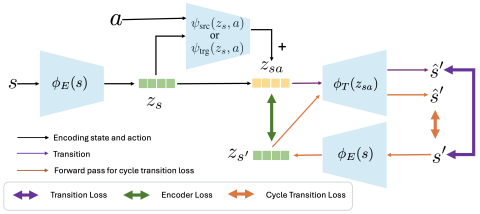

Figure 2: Architecture of the dynamics model. MOBODY encodes the state with ϕ_E and state action with ψ, outputs the next state through ϕ_T, and learns the dynamics for both domains by transition loss shown in purple double arrow ⇔. It learns the state action representation by matching the state action representation z_{sa} with the next state representation $z_{s'}$ through encoder loss shown in the green double arrow ⇔ and the state representation through cycle transition loss shown in orange double arrow ⇔.

3.1 Learning the Target Dynamics

Decomposition of the dynamics. In general, the dynamics can be modeled as $s' = \phi(s, a)$ or $s' = \phi^{\text{src}}(s, a)$ and $s' = \phi^{\text{trg}}(s, a)$ for the two domains. Although the dynamics are different, the transitions share some structured knowledge that we can utilize. Also, from another perspective, for the two domains, to achieve the same next state, different action is required, i.e., $(s, a_{\text{src}}, s')_{\text{src}}$ and $(s, a_{\text{trg}}, s')_{\text{trg}}$. Based on this, we propose using separate action encoders to encode actions from the two domains into the shared latent space. So the source and target domains can share a unified representation of states and a common transition function with the latent action.

We define the z_s as the state representation, z_{sa}^{src} and z_{sa}^{trg} as the state-action representations from the action encoder for source and target dynamics, respectively. Specifically, we model the state and state

action representation through $z_s = \phi_E(s)$, $z_{sa}^{\text{trg}} = \psi_{\text{trg}}(z_s, a)$ and $z_{sa}^{\text{src}} = \psi_{\text{src}}(z_s, a)$, so that we can obtain a separate state action representation for two domains. So, with the learned representation z_s and z_{sa}, we have the dynamics modeled as $s' = \phi_T(z_s, \psi(z_s, a))$, where ϕ_T is the transition function. For simplicity and to reduce the model parameters, we choose to directly add the state and state action representation together and feed into the transition function $s' = \phi_T(z_s + \psi(z_s, a))$. We show the flow of the dynamics learning component in Figure 2. And our dynamics model is:

$$\text{source dynamics} : z_s = \phi_E(s), z_{sa} = z_s + \psi_{\text{src}}(z_s, a), \hat{s}' = \phi_T(z_{sa}), \tag{1}$$

$$\text{target dynamics} : z_s = \phi_E(s), z_{sa} = z_s + \psi_{\text{trg}}(z_s, a), \hat{s}' = \phi_T(z_{sa}), \tag{2}$$

where ϕ_E is the state encoder, ϕ_T is the transition, and ψ_{src} and ψ_{trg} are the state action encoders for source and target, respectively. Equation (1) and Equation (2) show that we use different modules (action encoder ψ_{src} and ψ_{trg}) for the source and target domains, but with shared state representation from state encoder ϕ_E and unified transition function ϕ_T. We now discuss how representation learning techniques, utilizing several loss functions, enable us to learn representation and dynamics.

Transition Loss. The transition loss minimizes the Mean Squared Error of the predicted next state and the ground truth next state as shown in a purple two-way arrow in Figure 2. The goal of the transition loss is to learn the shared transition knowledge ϕ_T using both source and target data.

$$L_{\text{dyn}}^{\text{src}} = \frac{1}{N}\sum_{i=1}^{N} \|s' - \phi_T(z_s + \psi_{\text{src}}(z_s, a))\|^2; L_{\text{dyn}}^{\text{trg}} = \frac{1}{N}\sum_{i=1}^{N} \|s' - \phi_T(z_s + \psi_{\text{trg}}(z_s, a))\|^2. \tag{3}$$

Encoder Loss (Learning separate action encoder ψ_{src} and ψ_{trg}). The ϕ_T can map the latent state action representation to the next state for both domains, we use encoder loss to learn the separate action encoders for the two domains to map different actions to the unified latent space that served as the input to the ϕ_T. Specifically, we adopt a general assumption in representation learning that the representation of the state action should be close to the next state (Ye et al., 2021; Hansen et al., 2022b), where the predicted representation of the current state-action pair $\psi(s, a)$ incorporates the transition information to be close to the next state representation $\phi_E(s')$. This encourages the action encoder to further encode the difference of the dynamics information for the two domains, thereby improving the efficiency of learning the dynamics model. The encoder loss is formulated as:

$$L_{\text{rep}}^{\text{src}} = \frac{1}{N}\sum_{i=1}^{N} \||z_{s'}|_\times - (z_s + \psi_{\text{src}}(z_s, a))\|^2, L_{\text{rep}}^{\text{trg}} = \frac{1}{N}\sum_{i=1}^{N} \||z_{s'}|_\times - (z_s + \psi_{\text{trg}}(z_s, a))\|^2, \tag{4}$$

$z_{s'} = \phi_E(s')$ is the next state representation encoded with ϕ_E and $|\cdot|_\times$ is the stopping gradient. Here, N is the batch size. The encoder loss is shown in a green two-way arrow in Figure 2.

Cycle Transition Loss (Learning shared ϕ_E and ϕ_T). To further improve the state representation quality and avoid mode collapse in the encoder loss, we include a "cycle transition loss" through VAE-style (Kingma et al., 2013) learning. The dynamics function maps the state action to the next state through the state action representation. Then, from one perspective, by setting ψ to 0, the dynamics only input the state into the dynamics learning framework, and no action will be taken. The output of the dynamics will be the same state, i.e., $(s, 0, s)$, which is the same for two domains. So when the ψ is set to 0, the state is predicted as: $\hat{s} = \phi_T(\phi_E(s) + 0)$. Then we can explicitly learn the state representation with the state in the offline dataset by minimizing: $\|\phi_T(\phi_E(s)) - s\|_2$. From this perspective, we can view ϕ_E as an encoder and ϕ_T as a decoder, and we propose using a Variational AutoEncoder (VAE) (Kingma et al., 2013) to learn the state representation.

Let z_s be expressed as $z_s = \mu_{\phi_E}(s) + \sigma_{\phi_E}(s) \odot \epsilon$, with $\epsilon \sim \mathcal{N}(0, I)$ and $\mu_{\phi_E(s)}$ and σ_{ϕ_E} are the output of state encoder network ϕ_E. Let d_z be the dimension of the latent representation, the loss for learning the state representation is:

$$\mathcal{L}_{\text{cycle}} = \frac{1}{2N}\sum_{i=1}^{N}\sum_{j=1}^{d_z}\left(\mu_{i,j}^2 + \sigma_{i,j}^2 - \log\sigma_{i,j}^2 - 1\right) + \frac{1}{N}\sum_{i=1}^{N}\|s_i - \hat{s}_i\|_2, \tag{5}$$

The cycle transition loss is shown in an orange two-way arrow in Figure 2.

Unlike previous VAE-based dynamics learning methods, which are not tailored for off-dynamics RL, we introduce a cycle transition loss alongside the encoder loss to jointly learn state representations and shared transition functions across domains, rather than just learning state representations. The VAE representation also mitigates mode collapse that arises when trained solely on the encoder loss. The decoder, serving as a shared transition function, maps the unified state-action representation from separate action encoders to the next state, providing additional supervision signals for learning cross-domain dynamics. In conclusion, our method learns the unified transition function ϕ_T for both domains, while using the ψ_{src} and ψ_{trg} to learn the distinct information of the two dynamics.

Reward learning and uncertainty quantification (UQ) of the learned dynamics. Given that the reward is modeled as a function of (s, a, s') tuple and the reward function is the same across domains, we learn the reward function $\hat{r}(s, a, s')$ as a function of the (s, a, s') tuple with the combined source and target dataset through the MSE loss L_{reward}. This is further described in the Appendix B. Also, we follow the standard model-based approach (Yu et al., 2020) for the UQ of the dynamics, by penalizing the estimated reward $\hat{r}$ with the uncertainty in predicting the next state: $\tilde{r}(s, a, s') = \hat{r}(s, a, s') - \beta u(s, a)$ where $u(s, a)$ the uncertainty of the next state and β is the scale parameter. We refer to the details in Appendix B.

To summarize, the dynamics learning loss is:

$$\min \mathbb{E}_{D_{\text{src}}} L^{\text{src}}_{\text{dyn}} + \mathbb{E}_{D_{\text{trg}}} L^{\text{trg}}_{\text{dyn}} + \mathbb{E}_{D_{\text{src}} \cup D_{\text{trg}}} [L_{\text{reward}} + \lambda_{\text{rep}}(L_{\text{cycle}} + L_{\text{rep}})], \tag{6}$$

where λ_{rep} is a scalar that controls the weight of the representation learning term and is set to be 1 in the experiments, as we notice there is no significant performance difference with different λ_{rep}. We summarize the dynamics learning algorithm in Algorithm 1.

3.2 Policy Learning with the Target-Q-Weighted Behavior Cloning Loss

After we learn the target dynamics, we perform model-based offline RL training. During the policy optimization, we roll out new target data from the learned *target* dynamics with the current policy and state in the offline data and keep the rollout data in the $\mathcal{D}_{\text{fake}}$. Also, we want to utilize the source data to optimize the policy. We follow the previous work by DARA (Liu et al., 2022) on off-dynamics offline RL. This approach first performs reward regularization on the source data, which learns domain classifiers to penalize the large shift in the source data. Details of the DARA are referred to in Appendix C.1. Our *enhanced target data* is $\mathcal{D}_{\text{src\_aug}} \cup \mathcal{D}_{\text{trg}} \cup \mathcal{D}_{\text{fake}}$.

Learning the Q function We learn the Q functions following standard temporal difference learning with *enhanced target data*:

$$\min \mathcal{L}_{\text{Q}} = \min \mathbb{E}_{\mathcal{D}_{\text{src\_aug}} \cup \mathcal{D}_{\text{trg}} \cup \mathcal{D}_{\text{fake}}} \left[\left(r + \gamma \max_{a'} Q_{\theta^-}(s', a') - Q_\theta(s, a) \right)^2 \right]. \tag{7}$$

Policy optimization with target Q-weighted behavior cloning. In offline RL, a central challenge is exploration error, as out-of-distribution actions cannot be reliably evaluated—an issue exacerbated under off-dynamics settings. Behavior cloning (Fujimoto & Gu, 2021; Goecks et al., 2019) offers a simple and effective regularization by biasing the policy toward actions in the offline dataset, by pushing actions close to the actions in the offline dataset. However, in off-dynamics RL, naively cloning source-domain actions can harm performance: actions in the source dataset may perform poorly in the target domain due to the dynamics shift, so vanilla behavior cloning alone in TD3-BC (Fujimoto & Gu, 2021) is insufficient for policy regularization.

Instead, inspired by the advantage weighted regression and the IQL (Kostrikov et al., 2021a), i.e. $L_\pi(\phi) = \mathbb{E}_{(s,a)\sim\mathcal{D}} \left[\exp\left(\beta \left(\hat{Q}_\theta(s, a) - V_\psi(s)\right)\right) \log \pi_\phi(a \mid s) \right]$, which re-weight the log likelihood of the offline data with the advantage, we can re-weight the behavior cloning loss with the *target* Q value, namely a Q weighted behavior cloning loss, where the target Q value is learned with *enhanced target data*, so that this Q value approximates the Q value in the target domain. Intuitively, the target Q-weighted behavior cloning loss up-weights the policy's loss with higher target Q-values, guiding the policy toward actions expected to perform better under target dynamics. The policy loss with Q weighted behavior cloning loss is:

$$\begin{aligned} \pi = \arg\min_\pi & -\mathbb{E}_{(s,a)\in D_{\text{src\_aug}} \cup D_{\text{trg}} \cup D_{\text{fake}}} \left[\lambda Q(s, \pi(s)) \right] \\ & + \mathbb{E}_{(s,a)\in D_{\text{src\_aug}} \cup D_{\text{trg}}} \left[\exp\left(\frac{Q(s, \pi(s))}{1/N \sum_i^N |Q(s_i, \pi(s_i))|} \right) (\pi(s) - a)^2 \right], \end{aligned} \tag{8}$$

where the $\lambda = \frac{\alpha}{1/N \sum_i^N |Q(s,a)|}$ is the scaler λ that balance the behavior regularization error and Q loss and α is a hyper parameters. We summarize the MOBODY in Algorithm 2 in the Appendix B.

4 Experiments

In this section, we empirically evaluate MOBODY in off-dynamics offline RL settings using four MuJoCo environments from the ODRL benchmark: HalfCheetah-v2, Ant-v2, Walker2d-v2, and Hopper-v2 and manipulation tasks in Adroit: Pen and Door. We also perform comprehensive ablation studies to justify the importance of each component of MOBODY.

4.1 EXPERIMENTAL SETUP

Environments, Tasks, and Datasets. We evaluate MOBODY on the MuJoCo and Adroit environments from the ODRL benchmark (Lyu et al., 2024b). For the MuJoCo environment, we set the source domain unchanged and consider several types of dynamics shifts for the target domain, 1) gravity and friction, each scaled at four levels: $\{0.1, 0.5, 2.0, 5.0\}$ by multiplying the original values in MuJoCo, and 2) kinematics and morphology shift, each is achieved by constraining the rotation angle ranges of certain joints or modifying the size of specific limbs or the torsos of the robot. We also consider the Adroit task with kinematics and morphology shift, scaled to medium and hard shift levels, to demonstrate that our method applies to a wide range of environments and shift types/levels. We use the medium-level offline datasets collected by the ODRL benchmark, using an SAC-trained behavior policy tuned to achieve about 50% of expert performance. The target data contains only 5,000 transitions, whereas the source data contains 1 million transitions.

We evaluate the performance with the **Normalized Score**, defined as: $normalized\_score = \frac{score - random\_score}{expert\_score - random\_score} \times 100$, where the $random\_score$ is achieved by the random policy and the $expert\_score$ is achieved by the SAC (Haarnoja et al., 2018) trained to the expert level in the target domain. We also conduct hyperparameter and computational cost analysis in the Appendix C.4 to demonstrate that our method is not overly sensitive to hyperparameters.

Baselines. We compare MOBODY with several baseline methods, including the model-free offline RL algorithms, model-based offline RL algorithms, and off-dynamics offline RL algorithms. For the model-free offline RL methods, we choose the IQL (Kostrikov et al., 2021a) and TD3-BC (Fujimoto & Gu, 2021) as they demonstrate good performance without any modification designed for solving off-dynamics offline RL problems. We directly train these baselines on the combined offline dataset with the source and target data. We select the MOPO (Yu et al., 2020) as the model-based offline RL baselines. Since directly training dynamics on the target domain has poor performance, we train the dynamics model of MOPO on the combined dataset and train the RL policy with the dynamics model and the combined dataset, which is also a widely used model-based baseline in previous off-dynamics RL works (Eysenbach et al., 2020). We also incorporate the well-established off-dynamics offline RL methods, including DARA (Liu et al., 2022) and BOSA (Liu et al., 2024). We also conduct experiments comparing with different dynamics learning methods in Section 4.4.

4.2 MAIN RESULTS

Result on MuJoco gravity/friction shift. In Table 1, we show the detailed results and highlight the best and second-best scores of the MuJoco gravity and friction shift problems. In the last column, we report the percentage improvement or drop of our method compared to the best-performing baseline. Our proposed MOBODY outperforms baselines in 28 out of 32 settings, with competitive performance in the remaining four.

In detail, our MOBODY achieves 58.35% improvements compared with the best baseline methods, which is significantly better than the baselines and significantly outperforms baselines in hard settings, where other methods achieve extremely poor performance. In the last row of Table 1, we sum the normalized scores in total. We find that DARA and BOSA do not have significant improvements compared with IQL, and IQL achieves the best performance among the baselines in the total score. These empirical results underscore the superior performance of MOBODY in solving the off-dynamics offline RL problem and the potential in real-world applications where dynamics shifts are large.

Result on MuJoco kinematics/morphology shift. We also conduct experiments on MuJoco and Adroit with kinematics shift and morphology shift. Due to page limit, we summarize the results in Figure 3 by summing the normalized score across different tasks. We observe that MOBODY receives a higher overall score. We also present all the experimental results for each task in Table 4 and Table 5 in Appendix C.3, showing that our method performs the best in 32 out of 40 tasks and achieves an overall 25% improvement in all tasks.

MOBODY improves more when the dynamics shift is larger. Additionally, in larger shift scenarios, such as HalfCheetah-Friction-0.1, Ant-Friction-5.0, and Walker2d-Friction-5.0, MOBODY achieves significant improvement over baseline methods, which receive very low rewards in the target domain. We also summarize the performance comparison under different shift levels in Figure 4 in Appendix C.3. Existing methods, DARA and BOSA, fail in large shift settings as the reward

Table 1: Performance of MOBODY and baselines on MuJoCo tasks (HalfCheetah, Ant, Walker2D, Hopper) under medium-level offline dataset with dynamics shifts in gravity and friction at levels $0.1, 0.5, 2.0, 5.0$. Source domains remain unchanged; target domains are shifted. We report normalized target-domain scores (mean $\pm$ std over three seeds). Improvements are marked in $\uparrow$ and degradations in $\downarrow$ in the last column. Best and second-best scores are highlighted in **cyan** and **light cyan**, respectively.

Env	Level	BOSA	IQL	TD3-BC	MOPO	DARA	MOBODY	$\uparrow\downarrow$
HalfCheetah Gravity	0.1	9.31 ± 1.94	9.62 ± 4.27	6.90 ± 0.34	6.28 ± 0.22	12.90 ± 1.01	**14.18 ± 1.06**	9.92%↑
	0.5	43.96 ± 5.68	44.23 ± 2.93	6.38 ± 3.91	40.20 ± 7.20	46.11 ± 1.93	**47.18 ± 1.23**	2.32%↑
	2.0	27.86 ± 0.94	31.34 ± 1.68	29.29 ± 3.62	21.89 ± 10.49	31.85 ± 1.31	**41.60 ± 7.35**	30.61%↑
	5.0	17.95 ± 11.97	44.00 ± 23.13	73.75 ± 14.11	57.75 ± 18.92	27.67 ± 17.01	**83.05 ± 1.21**	12.61%↑
HalfCheetah Friction	0.1	12.53 ± 3.61	26.39 ± 11.35	8.95 ± 0.71	28.32 ± 9.23	23.69 ± 16.46	**57.53 ± 2.49**	103.14%↑
	0.5	68.93 ± 0.35	**69.80 ± 0.64**	49.43 ± 9.91	54.98 ± 5.91	64.89 ± 3.04	69.54 ± 0.48	0.37%↓
	2.0	46.53 ± 0.37	46.04 ± 2.04	43.51 ± 0.74	42.33 ± 3.89	46.25 ± 2.36	**50.02 ± 3.26**	45.00%↑
	5.0	44.07 ± 9.07	44.96 ± 6.78	35.83 ± 6.65	42.39 ± 10.22	40.06 ± 7.87	**59.20 ± 4.91**	31.67%↑
Ant Gravity	0.1	25.58 ± 2.21	12.53 ± 1.11	13.23 ± 2.61	8.93 ± 1.23	11.03 ± 1.24	**37.09 ± 2.12**	45.00%↑
	0.5	19.03 ± 4.41	10.09 ± 2.00	12.91 ± 2.85	12.28 ± 3.88	9.04 ± 1.35	**37.44 ± 2.79**	96.74%↑
	2.0	41.77 ± 1.52	37.17 ± 0.96	34.04 ± 4.12	35.43 ± 3.22	36.64 ± 0.82	**45.83 ± 1.71**	9.72%↑
	5.0	31.94 ± 0.69	31.59 ± 0.35	6.37 ± 0.45	28.97 ± 5.93	31.01 ± 0.39	**65.45 ± 3.23**	104.92%↑
Ant Friction	0.1	**58.95 ± 0.71**	55.56 ± 0.46	49.20 ± 2.55	49.86 ± 5.99	55.12 ± 0.24	58.79 ± 0.11	0.27%↓
	0.5	59.72 ± 3.57	59.28 ± 0.80	25.21 ± 7.17	32.28 ± 3.25	58.92 ± 0.80	**62.41 ± 4.10**	4.50%↑
	2.0	20.18 ± 3.79	19.84 ± 3.20	22.69 ± 8.10	15.93 ± 0.87	17.54 ± 2.47	**47.41 ± 4.40**	108.95%↑
	5.0	9.07 ± 0.88	7.75 ± 0.25	10.06 ± 4.16	13.89 ± 3.2	7.80 ± 0.12	**31.17 ± 5.57**	124.41%↑
Walker2d Gravity	0.1	18.75 ± 12.02	16.04 ± 7.60	36.48 ± 0.95	41.98 ± 10.13	20.12 ± 5.74	**65.85 ± 5.08**	56.86%↑
	0.5	40.09 ± 20.37	42.05 ± 10.52	27.43 ± 3.92	40.32 ± 8.78	29.72 ± 16.02	**43.57 ± 2.32**	3.61%↑
	2.0	8.91 ± 2.28	25.69 ± 10.70	11.88 ± 9.38	28.79 ± 3.07	32.20 ± 1.05	**44.32 ± 4.58**	37.64%↑
	5.0	5.25 ± 0.50	5.42 ± 0.29	5.12 ± 0.18	5.65 ± 0.99	5.44 ± 0.08	**46.05 ± 20.73**	715.04%↑
Walker2d Friction	0.1	7.88 ± 1.88	5.72 ± 0.23	**29.60 ± 24.90**	27.99 ± 2.11	5.65 ± 0.06	28.23 ± 9.13	4.63%↓
	0.5	63.94 ± 20.40	66.26 ± 3.03	45.01 ± 18.98	60.81 ± 3.04	68.81 ± 1.12	**76.96 ± 1.99**	11.84%↑
	2.0	39.06 ± 17.36	65.40 ± 7.13	67.89 ± 1.66	68.38 ± 1.09	72.91 ± 0.37	**73.74 ± 0.49**	1.14%↑
	5.0	10.07 ± 4.91	5.39 ± 0.03	5.76 ± 0.84	5.34 ± 1.61	5.36 ± 0.28	**27.38 ± 3.87**	171.90%↑
Hopper Gravity	0.1	27.82 ± 13.41	13.10 ± 0.98	15.59 ± 6.09	22.49 ± 3.71	23.40 ± 11.62	**36.25 ± 1.50**	30.30%↑
	0.5	28.54 ± 12.77	16.24 ± 7.89	23.00 ± 14.87	23.92 ± 1.91	12.86 ± 0.18	**33.57 ± 6.71**	17.62%↑
	2.0	11.84 ± 2.37	16.10 ± 1.64	18.62 ± 6.88	11.76 ± 0.32	14.65 ± 2.47	**23.79 ± 2.09**	27.77%↑
	5.0	7.36 ± 0.13	8.12 ± 0.16	**9.08 ± 1.15**	7.77 ± 0.31	7.90 ± 1.27	8.06 ± 0.03	11.23%↓
Hopper Friction	0.1	25.55 ± 2.69	24.16 ± 4.50	18.64 ± 3.37	34.32 ± 6.79	26.13 ± 4.24	**51.19 ± 2.56**	49.16%↑
	0.5	25.22 ± 4.48	23.56 ± 1.68	19.60 ± 15.45	12.32 ± 3.96	26.94 ± 2.86	**41.34 ± 0.49**	53.45%↑
	2.0	10.32 ± 0.06	10.15 ± 0.06	9.89 ± 0.20	10.99 ± 0.76	10.15 ± 0.03	**11.00 ± 0.14**	0.09%↑
	5.0	7.90 ± 0.06	7.93 ± 0.01	7.80 ± 1.04	7.68 ± 0.19	7.86 ± 0.05	**8.07 ± 0.04**	1.77%↑
Total		875.88	901.52	779.14	893.22	890.62	**1427.26**	58.35%↑

regularization methods are mainly trained with source data with regularization, resulting in optimizing the policy with the low dynamics-shift transitions and cannot adapt to the large shift target domain, as we mentioned earlier. Thus, such methods lack exploration of high-reward states in the target domain that do not fall within these low dynamics-shift regions, which is more frequent when shift is large.

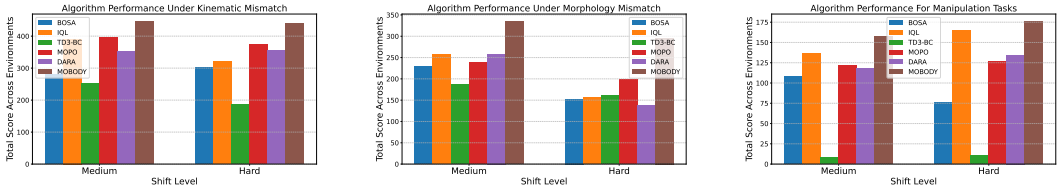

(a) Kinematic Shift (b) Morphology Shift (c) Manipulation Task

Figure 3: Aggregation experimental results on MuJoco kinematic and morphology shift task, and Manipulation tasks. Our method outperforms the baselines. Detailed results of each environment, shift type, and shift level are referred to Table 4 and Table 5 in the Appendix C.3.

4.3 Ablation Study

In this section, we conduct ablation studies on two main components of MOBODY: dynamics learning and policy learning. We first evaluate the overall effectiveness of each component, then analyze specific design choices. For dynamic learning, we assess the impact of the cycle transition loss and representation learning. For policy learning, we examine the effectiveness of the Q-weighted loss.

We evaluate on the Walker2d environments as discussed in Section 4.1. The ablation study results are shown in Table 2. We defer more ablation study results on Hopper to Appendix C.4.

We first evaluate the performance of our proposed dynamics learning and policy learning by replacing the dynamics learning with the existing dynamics learning model or the policy learning with the existing offline RL algorithm. We denote the two ablation studies as follows:

A1: Replace dynamics learning We compare our MOBODY with a variant replacing the dynamics learning with the existing model-based method. We use a black-box dynamics model trained on **target data only**, while the policy learning follows the same method as in MOBODY. Table 2 demonstrates that the **A1** variant is significantly degraded compared with our proposed MOBODY algorithm in Walker2d. This indicates that only using the existing dynamics models trained on the target data is insufficient to rollout trajectories in the target domain. This motivates us to propose a novel dynamics model learning method.

A2: Replace policy learning Similar to the **A1**, we replace the policy learning with the existing offline RL algorithm. We adopt the same dynamics learning approach as in MOBODY and use Conservative Q-Learning (CQL) (Kumar et al., 2020) for policy learning. Table 2 shows that our proposed MOBODY outperforms the **A2** variant in Walker2d. This demonstrates that the policy learning part of our proposed MOBODY with Q-weight behavior cloning can better utilize the dynamics model compared with the existing method.

Then we delve into the details of the dynamics learning and policy learning part, especially our designs of the loss function and Q-weighting. We have the following ablation studies:

A3: No Cycle Transition Loss Here, the dynamics model follows the dynamics learning of the proposed MOBODY, but without the cycle transition loss. We hope to evaluate the effectiveness of our proposed cycle transition loss. Table 2 illustrates that the **A3** suffers degradations compared with our MOBODY in most of the settings. This indicates that the cycle transition loss helps learn a better state representation in our proposed MOBODY method.

A4: No Q-weighted Similar to the **A3**, we compare our MOBODY with a variant without the Q-weighted behavior cloning loss. We keep the same dynamics learning method as our proposed MOBODY and replace the Q-weighted behavior cloning loss with the vanilla behavior cloning loss. In Table 2, our method outperforms the method without the Q-weighted behavior cloning in Walker2d. The **A4** underperforms MOBODY in most of the settings except the Walker2d 2.0 level, where all settings have similar performance. This suggests that our proposed Q-weighted approach can help regularize the policy learning in the off-dynamics offline RL scenarios.

Table 2: Performance of the ablation study of our proposed MOBODY method. A1-A4 represent four different ablation studies detailed in Section 4.3. The experiments are conducted on the Walker2d environments under the medium-level with dynamics shifts in gravity and friction in $\{0.1, 0.5, 2.0, 5.0\}$ shift levels. The source domains are the original environments, and the target domains are the environments with dynamic shifts. We report the normalized scores in the target domain with the mean and standard deviation across three random seeds. The higher scores indicate better performance.

Env	Level	Algorithm Ablation		Loss Ablation		MOBODY
		A1	A2	A3	A4	
Walker2d Gravity	0.1	55.23 ± 10.22	55.43 ± 5.31	35.34 ± 10.97	19.53 ± 4.68	65.85 ± 5.08
	0.5	35.66 ± 3.11	39.98 ± 1.32	30.63 ± 2.92	24.44 ± 1.91	43.57 ± 2.32
	2.0	31.94 ± 5.32	28.58 ± 5.59	34.42 ± 3.60	47.13 ± 2.44	44.32 ± 4.58
	5.0	3.56 ± 0.79	11.37 ± 3.91	4.42 ± 1.20	6.43 ± 0.32	46.05 ± 20.73
Walker2d Friction	0.1	24.34 ± 10.33	25.73 ± 2.43	21.42 ± 3.85	19.48 ± 4.32	28.23 ± 9.13
	0.5	56.31 ± 7.17	73.23 ± 3.73	68.53 ± 4.14	61.38 ± 6.84	76.96 ± 1.99
	2.0	60.52 ± 5.82	71.14 ± 2.59	67.98 ± 6.96	76.44 ± 6.43	73.74 ± 0.49
	5.0	4.32 ± 0.85	18.32 ± 2.18	5.42 ± 0.82	7.89 ± 1.33	27.38 ± 3.87

4.4 COMPARISON AMONG DIFFERENT DYNAMICS LEARNING APPROACHES

As a model-based approach, MOBODY's learned target dynamics is capable of generating higher quality transitions and demonstrates superior estimation error. Here we compare our MOBODY with model-based approaches with different dynamics learning baselines, including **1)** target only: learning dynamics with target data only, **2)** combined data: learning dynamics with combined source and target data, and **3)** pretrain-finetune learning the dynamics by first pretrain dynamics with source data and then finetune it with the target dataset. For a fair comparison in terms of dynamics learning, we use the same model architecture as MOBODY, except that we use the same action encoder for both domains and we do not use a cycle transition loss. We also evaluate the learned dynamics model with the MSE of the rollout trajectories using the policy learned by MOBODY at different steps (0.25M, 0.5M, 0.75M and 1M steps).

Table 3: Performance comparison using different dynamics learning models. First row: evaluation MSE of the rollout trajectories using different MOBODY policy, second row: normalized score of the policy. We see that MOBODY outperforms the baseline dynamics learning methods in both dynamics learning and overall performance.

Metric	Task	Trained only on target data	Combined data	Pretrained-finetune	MOBODY
MSE	Walker2d-friction-0.5	2.23 ± 0.26	1.96 ± 0.68	2.21 ± 0.19	$\mathbf{1.25 \pm 0.39}$
	Walker2d-gravity-0.5	2.11 ± 0.48	1.87 ± 0.32	2.32 ± 0.23	$\mathbf{1.93 \pm 0.34}$
	Ant-friction-0.5	2.99 ± 0.51	2.01 ± 0.24	2.14 ± 0.19	$\mathbf{1.88 \pm 0.18}$
	Ant-gravity-0.5	1.57 ± 0.39	1.53 ± 0.39	1.73 ± 0.43	$\mathbf{1.46 \pm 0.26}$
Normalized Score	Walker2d-friction-0.5	56.31 ± 7.17	41.38 ± 5.12	62.93 ± 5.43	$\mathbf{76.96 \pm 1.99}$
	Walker2d-gravity-0.5	39.71 ± 3.29	42.13 ± 3.98	38.13 ± 3.12	$\mathbf{43.57 \pm 2.32}$
	Ant-friction-0.5	48.13 ± 4.43	46.23 ± 6.85	51.09 ± 1.93	$\mathbf{62.41 \pm 4.10}$
	Ant-gravity-0.5	28.32 ± 3.87	31.39 ± 3.80	29.69 ± 7.23	$\mathbf{37.44 \pm 2.79}$

Table 3 shows the policy optimization performance and the evaluation MSE of the different learned dynamics. We can observe that the proposed MOBODY outperforms the baseline dynamics learning methods. The reason can be summarized as follows: 1) the target only dataset is very small, thus not sufficient to learn the dynamics well, 2) the dynamics learned by the combined dataset can be biased towards a dynamics in between the source and target domains, and 3) pretrain-finetune training paradigm treat source and target domains using the same model but does not capture the difference and the shared structure of the two domains. Specifically, although the pretrain–finetune paradigm has achieved notable success in supervised domain adaptation tasks, such as domain-adaptive image classification, it is less effective in the off-dynamics RL setting. In image classification, it is possible to first extract a broad range of features through pretraining from the source and then finetune on the target domain to focus on generalizable features. However, when learning the dynamics, the learning target, which is the next state s' conditioned on (s, a), differs fundamentally across domains. This mismatch makes it difficult to directly adapt to the target domain through finetuning alone, without explicitly considering the difference in the dynamics model of the two domains in the initial representation learning. Thus, our method seeks to learn the shared information for both domains, while also learn the separate action encoder to account for the dynamics difference across domains.

5 CONCLUSION

In this work, we study the off-dynamics offline reinforcement learning problem through a model-based offline RL method. We introduce MOBODY, a model-based offline RL algorithm that enables policy exploration in the target domain via learned dynamics models. By leveraging shared latent representations across domains, MOBODY effectively learns target dynamics using both source and limited target data. Additionally, we propose a Q-weighted behavior cloning strategy that favors actions with high target Q value, further improving policy learning. Experimental results on MuJoCo and Adroit benchmarks demonstrate that MOBODY consistently outperforms prior methods, particularly in scenarios with significant dynamic mismatches, highlighting its robustness and generalization capabilities. Our method shows the potential of data augmentation in policy learning with a carefully learned dynamics model. Future work includes further investigation on improving the dynamics learning.

REPRODUCIBILITY STATEMENT

Our codes are available at: https://anonymous.4open.science/r/off-dynamics-model-based-rl-D53D/README.md. The implementation of the method is based on the ODRL benchmark repository (Lyu et al., 2024b), which provides the comprehensive dataset and baseline method for evaluation. For our algorithm, we provide detailed information on the training loss for the dynamics learning and the policy optimization in the main text as well as the Algorithm 1 for dynamics learning and Algorithm 2 for policy optimization in Appendix B. We also provide hyperparameter analysis and rule-of-thumb hyperparameters in Appendix C.4, as well as the hyperparameters and model architecture that we used for tuning in Table 9.

REFERENCES

André Barreto, Will Dabney, Rémi Munos, Jonathan Hunt, Tom Schaul, David Silver, and Hado van Hasselt. Successor features for transfer in reinforcement learning. In *Advances in Neural Information Processing Systems*, volume 30, pp. 4055–4065, 2017.

Nicolò Botteghi, Mannes Poel, and Christoph Brune. Unsupervised representation learning in deep reinforcement learning: A review. *IEEE Control Systems*, 45(2):26–68, 2025.

Benjamin Eysenbach, Swapnil Asawa, Shreyas Chaudhari, Sergey Levine, and Ruslan Salakhutdinov. Off-dynamics reinforcement learning: Training for transfer with domain classifiers. *arXiv preprint arXiv:2006.13916*, 2020.

Scott Fujimoto and Shixiang Shane Gu. A minimalist approach to offline reinforcement learning. *Advances in neural information processing systems*, 34:20132–20145, 2021.

Scott Fujimoto, David Meger, and Doina Precup. A deep reinforcement learning approach to marginalized importance sampling with the successor representation. In *International Conference on Machine Learning*, pp. 3518–3529. PMLR, 2021.

Scott Fujimoto, Wei-Di Chang, Edward J Smith, Shixiang Shane Gu, Doina Precup, and David Meger. For sale: State-action representation learning for deep reinforcement learning. In *Advances in Neural Information Processing Systems*, 2023.

Vinicius G Goecks, Gregory M Gremillion, Vernon J Lawhern, John Valasek, and Nicholas R Waytowich. Integrating behavior cloning and reinforcement learning for improved performance in dense and sparse reward environments. *arXiv preprint arXiv:1910.04281*, 2019.

Yihong Guo, Yixuan Wang, Yuanyuan Shi, Pan Xu, and Anqi Liu. Off-dynamics reinforcement learning via domain adaptation and reward augmented imitation. In *Advances in Neural Information Processing Systems*, volume 37, pp. 136326–136360, 2024.

Tuomas Haarnoja, Aurick Zhou, Pieter Abbeel, and Sergey Levine. Soft actor-critic: Off-policy maximum entropy deep reinforcement learning with a stochastic actor. In *International conference on machine learning*, pp. 1861–1870. PMLR, 2018.

Nicklas Hansen, Xiaolong Wang, and Hao Su. Temporal difference learning for model predictive control. In *International Conference on Machine Learning (ICML)*, pp. 8387–8406. PMLR, 2022a.

Nicklas Hansen, Xiaolong Wang, and Hao Su. Temporal difference learning for model predictive control. *arXiv preprint arXiv:2203.04955*, 2022b.

Leslie Pack Kaelbling, Michael L Littman, and Andrew W Moore. Reinforcement learning: A survey. *Journal of artificial intelligence research*, 4:237–285, 1996.

Maximilian Karl, Maximilian Soelch, Justin Bayer, and Patrick van der Smagt. Deep variational bayes filters: Unsupervised learning of state space models from raw data. In *International Conference on Learning Representations (ICLR)*, 2017.

Rahul Kidambi, Aravind Rajeswaran, Praneeth Netrapalli, and Thorsten Joachims. Morel: Model-based offline reinforcement learning. *Advances in neural information processing systems*, 33: 21810–21823, 2020.

Diederik P Kingma, Max Welling, et al. Auto-encoding variational bayes, 2013.

B Ravi Kiran, Ibrahim Sobh, Victor Talpaert, Patrick Mannion, Ahmad A Al Sallab, Senthil Yogamani, and Patrick Pérez. Deep reinforcement learning for autonomous driving: A survey. *IEEE transactions on intelligent transportation systems*, 23(6):4909–4926, 2021.

Ilya Kostrikov, Ashvin Nair, and Sergey Levine. Offline reinforcement learning with implicit q-learning. *arXiv preprint arXiv:2110.06169*, 2021a.

Ilya Kostrikov, Denis Yarats, and Rob Fergus. Image augmentation is all you need: Regularizing deep reinforcement learning from pixels. In *International Conference on Learning Representations (ICLR)*, 2021b.

Aviral Kumar, Aurick Zhou, George Tucker, and Sergey Levine. Conservative q-learning for offline reinforcement learning. *Advances in neural information processing systems*, 33:1179–1191, 2020.

Hyeonhoon Lee, Hyun-Kyu Yoon, Jaewon Kim, Ji Soo Park, Chang-Hoon Koo, Dongwook Won, and Hyung-Chul Lee. Development and validation of a reinforcement learning model for ventilation control during emergence from general anesthesia. *npj Digital Medicine*, 6(1):145, 2023.

Sergey Levine, Aviral Kumar, George Tucker, and Justin Fu. Offline reinforcement learning: Tutorial, review, and perspectives on open problems. *arXiv preprint arXiv:2005.01643*, 2020.

Yuxi Li. Deep reinforcement learning: An overview. *arXiv preprint arXiv:1701.07274*, 2017.

Guoqing Liu, Chuheng Zhang, Li Zhao, Tao Qin, Jinhua Zhu, Jian Li, Nenghai Yu, and Tie-Yan Liu. Return-based contrastive representation learning for reinforcement learning. In *International Conference on Learning Representations (ICLR)*, 2021.

Jinxin Liu, Hongyin Zhang, and Donglin Wang. Dara: Dynamics-aware reward augmentation in offline reinforcement learning. *arXiv preprint arXiv:2203.06662*, 2022.

Jinxin Liu, Ziqi Zhang, Zhenyu Wei, Zifeng Zhuang, Yachen Kang, Sibo Gai, and Donglin Wang. Beyond ood state actions: Supported cross-domain offline reinforcement learning. In *Proceedings of the AAAI Conference on Artificial Intelligence*, volume 38, pp. 13945–13953, 2024.

Jiafei Lyu, Chenjia Bai, Jingwen Yang, Zongqing Lu, and Xiu Li. Cross-domain policy adaptation by capturing representation mismatch. *arXiv preprint arXiv:2405.15369*, 2024a.

Jiafei Lyu, Kang Xu, Jiacheng Xu, Jing-Wen Yang, Zongzhang Zhang, Chenjia Bai, Zongqing Lu, Xiu Li, et al. Odrl: A benchmark for off-dynamics reinforcement learning. *Advances in Neural Information Processing Systems*, 37:59859–59911, 2024b.

Kei Ota, Tomoaki Oiki, Devesh K Jha, Toshisada Mariyama, and Daniel Nikovski. Can increasing input dimensionality improve deep reinforcement learning? In *Proceedings of the 37th International Conference on Machine Learning*, pp. 7424–7433. PMLR, 2020.

Wendy S Parker. Ensemble modeling, uncertainty and robust predictions. *Wiley interdisciplinary reviews: Climate change*, 4(3):213–223, 2013.

Jan Peters and Stefan Schaal. Reinforcement learning by reward-weighted regression for operational space control. In *Proceedings of the 24th international conference on Machine learning*, pp. 745–750, 2007.

Paria Rashidinejad, Banghua Zhu, Cong Ma, Jiantao Jiao, and Stuart Russell. Bridging offline reinforcement learning and imitation learning: A tale of pessimism. *Advances in Neural Information Processing Systems*, 34:11702–11716, 2021.

Marc Rigter, Bruno Lacerda, and Nick Hawes. Rambo-rl: Robust adversarial model-based offline reinforcement learning. *Advances in neural information processing systems*, 35:16082–16097, 2022.

Ruhan Wang, Yu Yang, Zhishuai Liu, Dongruo Zhou, and Pan Xu. Return augmented decision transformer for off-dynamics reinforcement learning. 2024.

Xiaoyu Wen, Chenjia Bai, Kang Xu, Xudong Yu, Yang Zhang, Xuelong Li, and Zhen Wang. Contrastive representation for data filtering in cross-domain offline reinforcement learning. *arXiv preprint arXiv:2405.06192*, 2024.

Kang Xu, Chenjia Bai, Xiaoteng Ma, Dong Wang, Bin Zhao, Zhen Wang, Xuelong Li, and Wei Li. Cross-domain policy adaptation via value-guided data filtering. *Advances in Neural Information Processing Systems*, 36:73395–73421, 2023.

Denis Yarats, Rob Fergus, Alessandro Lazaric, and Lerrel Pinto. Mastering visual continuous control: Improved data-augmented reinforcement learning. In *International Conference on Learning Representations (ICLR)*, 2022.

Weirui Ye, Shaohuai Liu, Thanard Kurutach, Pieter Abbeel, and Yang Gao. Mastering atari games with limited data. *Advances in neural information processing systems*, 34:25476–25488, 2021.

Tianhe Yu, Garrett Thomas, Lantao Yu, Stefano Ermon, James Y Zou, Sergey Levine, Chelsea Finn, and Tengyu Ma. Mopo: Model-based offline policy optimization. *Advances in Neural Information Processing Systems*, 33:14129–14142, 2020.

Tianhe Yu, Aviral Kumar, Rafael Rafailov, Aravind Rajeswaran, Sergey Levine, and Chelsea Finn. Combo: Conservative offline model-based policy optimization. *Advances in neural information processing systems*, 34:28954–28967, 2021.

Jinhua Zhu, Yingce Xia, Lijun Wu, Jiajun Deng, Wengang Zhou, Tao Qin, and Houqiang Li. Masked contrastive representation learning for reinforcement learning. In *Advances in Neural Information Processing Systems (NeurIPS)*, 2020.

A Related Work

Off-dynamics RL. Off-dynamics RL aims to transfer the policy learned in the source domain to the target domain. One line of work is to regularize the reward of the source data with the target data using the domain classifier. Following this idea, DARC (Eysenbach et al., 2020) and DARAIL (Guo et al., 2024) solve the off-dynamics RL problem in the online paradigm, while DARA (Liu et al., 2022) and RADT (Wang et al., 2024) use the reward regularization techniques in the offline RL setting. Similarly, BOSA (Liu et al., 2024) regularizes the policy by two support-constrained objectives. PAR (Lyu et al., 2024a) learns the representation to measure the deviation of dynamic mismatch via the state and state-action encoder to modify the reward. Another line of work is utilizing the data filter method, including the VGDF (Xu et al., 2023) and IGDF (Wen et al., 2024), which filter out the trajectories similar to the target domain and train the RL policies on filtered data. These data filtering or reward regularization methods in off-dynamics offline RL settings cannot explore the target domain substantially, while we propose a novel model-based method that can explore the target domain with the learned *target* dynamics.

Model-based Offline RL. Model-based offline RL leverages the strengths of model-based methods in the offline RL paradigm. MOReL (Kidambi et al., 2020) and MOPO (Yu et al., 2020) modify reward functions based on uncertainty estimations derived from ensembles of models. VI-LCB (Rashidinejad et al., 2021) leverages pessimistic value iteration, incorporating penalty functions into value estimation to discourage poorly-covered state-action pairs. COMBO (Yu et al., 2021) provides a conservative estimation without explicitly computing uncertainty, using adversarial training to optimize conservative value estimates. RAMBO (Rigter et al., 2022) further builds upon adversarial techniques by directly training models adversarially with conservatively modified dynamics to reduce distributional shifts. These methods are designed for one domain instead of an off-dynamics RL setting. In this paper, we propose a novel dynamics learning and policy optimization method for an off-dynamics RL setting.

Representation Learning in RL. Representation learning (Botteghi et al., 2025) is actively explored in image-based reinforcement learning tasks (Kostrikov et al., 2021b; Yarats et al., 2022; Liu et al., 2021; Zhu et al., 2020) to learn the representation of the image. For model-based RL, to improve sample efficiency, representation has been widely applied to learn the latent dynamics modeling (Karl et al., 2017; Hansen et al., 2022a), latent state representation learning (Barreto et al., 2017; Fujimoto et al., 2021), or latent state-action representation learning (Ye et al., 2021; Hansen et al., 2022b; Ota et al., 2020; Fujimoto et al., 2023). In our paper, we learn the shared representation of the state and transition to auxiliary the *target* dynamics learning with source domain data.

B Algorithm Details

Reward learning Note that the reward is modeled as a function of (s, a, s') tuple, as in many tasks, the reward is also related to the next state as mentioned in the Section 2. Also, recall that the reward function in the source and target domain remains the same. Thus, we can learn the reward function with source and target domain data together via the following loss function.

$$L_{\text{reward}} = \frac{1}{2}\mathbb{E}_{D_{\text{src}}\cup D_{\text{trg}}}\left[r(s,a,s') - \hat{r}(s,a,s')\right]^2 + \frac{1}{2}\mathbb{E}_{D_{\text{src}}\cup D_{\text{trg}}}\left[r(s,a,s') - \hat{r}(s,a,\hat{s}')\right]^2, \tag{9}$$

where $\hat{s}'$ is the predicted next state. Here, we use both the true next state and the predicted next state from the dynamics model to learn the reward model, as during inference, we do not have the true next state and only have a predicted next state.

Uncertainty quantification (UQ) of the transition To capture the uncertainty of the model, we learn N ensemble transition models, with each model trained independently via Eq.equation 6. We design the UQ of the reward estimation as $u(s,a) := \max_i \text{Std}(\hat{s}'_j) = \max_i \sqrt{1/N \sum_{j=1}^{N} (\hat{s}'_j - \mathbb{E}(\hat{s}'))^2}$, which is the largest standard deviation among all the state dimensions. This simple and intuitive uncertainty quantification using the ensemble model has been proven simple and effective in many machine learning literature (Parker, 2013) and also model-based RL algorithms (Yu et al., 2020). We find it sufficient to achieve good performance in our experiments by employing the penalized reward $\tilde{r}$ for the downstream policy learning: $\tilde{r}(s,a,s') = \hat{r}(s,a,s') - \beta u(s,a)$.

Algorithm 1 Dynamics Learning via separate action encoders and the representation learning.

Input: Offline datasets $\mathcal{D}_{\text{src}} = \{(s, a, r, s')\}$, $\mathcal{D}_{\text{trg}} = \{(s, a, r, s')\}$, number of model learning steps N_{model}, target training frequency K.
Initialize: State encoder model ϕ_E, transition model ϕ_T, source state action encoder ψ_{src}, target state action encoder ψ_{trg}, reward model $\hat{r}$.
for $i = 1$ to N_{model} **do**
    Sample mini-batch:
    if $i\%K = 0$ **then**
        Sample mini-batch $\{(s, a, r, s')\}$ from $\mathcal{D}_{\text{trg}}$
    else
        Sample mini-batch $\{(s, a, r, s')\}$ from $\mathcal{D}_{\text{src}}$
    end if
    Predict the next state with Eq. equation 1, and equation 2 with mini-batch data.
    Optimize the dynamics with the transition loss in Eq.equation 3, encoder loss in Eq.equation 4, cycle transition loss in Eq.equation 5 and reward loss in Eq.equation 9 with mini-batch data.
end for

Algorithm 2 MOBODY: Model-Based Off-dynamics Offline Reinforcement Learning

Input: Offline dataset $\mathcal{D}_{\text{src}} = \{(s, a, r, s')\}$ and $\mathcal{D}_{\text{trg}} = \{(s, a, r, s')\}$, $D_{\text{fake}} = \{\}$, number of model learning steps N_{model}, policy training steps N_{policy}.
Initialize: Dynamics model, policy π_θ, rollout length L_{rollout}.
Dynamics Training
Learn target dynamics and reward estimation: $\hat{T}_{\text{trg}}, \hat{r}_{\text{trg}} \leftarrow$ Call Algorithm 1
Offline Policy Learning
Regularize source data $\mathcal{D}_{\text{src\_aug}} = \{(s, a, r + \eta\Delta r, s')\}$ with DARA.
for $j = 1$ to N_{policy} **do**
    Collect rollout data from $\hat{T}$ and $\hat{r}_{\text{trg}}$ starting from state in $D_{\text{src\_aug}}$ and D_{trg}. Add batch data to replay buffer D_{fake}.
    Sample batch $(s, a, s', r)_{\text{fake}}$ from $\mathcal{D}_{\text{fake}}$, $(s, a, s', r)_{\text{trg}}$ from $\mathcal{D}_{\text{trg}}$ and $(s, a, s', r)_{\text{trg\_aug}}$ from $\mathcal{D}_{\text{src\_aug}}$. Concatenate them as $(s, a, s', r)_{\text{train}}$.
    Learn the Q value function with Eq.equation 7
    Update policy π_θ with Eq. equation 8
end for
Return: Learned policy π_θ

C Experimental Details

C.1 The DARA Regularization for Source Data used in MOBODY

Note that in MOBODY, we use DARA to regularize the reward in the source data. In this section, we introduce the details of DARA.

DARA (Liu et al., 2022), the offline version of DARC (Eysenbach et al., 2020), trains the domain classifiers to calculate the reward penalty term $\Delta r(s, a, s')$ and regularize the rewards in the source domain dataset via:

$$\hat{r}_{\text{DARA}}(s, a, s') = r(s, a, s') + \eta \Delta r(s, a, s'),$$

where η is the penalty coefficient, where we set to 0.1 following the ODRL benchmark (Lyu et al., 2024b).

Estimation of the Δr. Following the DARC (Eysenbach et al., 2020; Liu et al., 2022), the reward regularization Δr can be estimated with the following two binary classifiers $p(\text{trg}|s_t, a_t)$ and $p(\text{trg}|s_t, a_t, s_{t+1})$ with Bayes' rules:

$$p(\text{trg}|s_t, a_t, s_{t+1}) = p_{\text{trg}}(s_{t+1}|s_t, a_t)p(s_t, a_t|\text{trg})p(\text{trg})/p(s_t, a_t, s_{t+1}), \tag{10}$$

$$p(s_t, a_t|\text{trg}) = p(\text{trg}|s_t, a_t)p(s_t, a_t)/p(\text{trg}). \tag{11}$$

Replacing the $p(s_t, a_t|\text{trg})$ in Eq. equation 10 with Eq. equation 11, we obtain:

$$p_{\text{trg}}(s_{t+1}|s_t, a_t) = \frac{p(\text{trg}|s_t, a_t, s_{t+1})p(s_t, a_t, s_{t+1})}{p(\text{trg}|s_t, a_t)p(s_t, a_t)}.$$

Similarly, we can obtain the $p_{\text{src}}(s_{t+1}|s_t, a_t) = \frac{p(\text{src}|s_t, a_t, s_{t+1})p(s_t, a_t, s_{t+1})}{p(\text{src}|s_t, a_t)p(s_t, a_t)}$.

We can calculate the $\Delta r(s_t, a_t, s_{t+1})$ following:

$$\begin{aligned}\Delta r(s_t, a_t, s_{t+1}) &= \log\left(\frac{p_{\text{trg}}(s_{t+1}|s_t, a_t)}{p_{\text{src}}(s_{t+1}|s_t, a_t)}\right) \\ &= \log p(\text{trg}|s_t, a_t, s_{t+1}) - \log p(\text{trg}|s_t, a_t) + \log p(\text{src}|s_t, a_t, s_{t+1}) - \log p(\text{src}|s_t, a_t).\end{aligned}$$

Training the Classifier $p(\textbf{trg}|s_t, a_t)$ and $p(\textbf{trg}|s_t, a_t, s_{t+1})$. The two classifiers are parameterized bu θ_{SA} and θ_{SAS}. To update the two classifiers, we sample one mini-batch of data from the source replay buffer D_{src} and the target replay buffer D_{src} respectively. Imbalanced data is considered here as each time we sample the same amount of data from the source and target domain buffer. Then, the parameters are learned by minimizing the standard cross-entropy loss:

$$\begin{aligned}\mathcal{L}_{\text{SAS}} &= -\mathbb{E}_{\mathcal{D}_{\text{src}}}\left[\log p_{\theta_{\text{SAS}}}(\text{trg}|s_t, a_t, s_{t+1})\right] - \mathbb{E}_{\mathcal{D}_{\text{trg}}}\left[\log p_{\theta_{\text{SAS}}}(\text{trg}|s_t, a_t, s_{t+1})\right], \\ \mathcal{L}_{\text{SA}} &= -\mathbb{E}_{\mathcal{D}_{\text{src}}}\left[\log p_{\theta_{\text{SA}}}(\text{trg}|s_t, a_t, s_{t+1})\right] - \mathbb{E}_{\mathcal{D}_{\text{trg}}}\left[\log p_{\theta_{\text{SA}}}(\text{trg}|s_t, a_t, s_{t+1})\right].\end{aligned}$$

Thus, $\theta = (\theta_{\text{SAS}}, \theta_{\text{SA}})$ is obtained from:

$$\begin{aligned}\theta &= \arg\min_{\theta} \mathcal{L}_{CE}(\mathcal{D}_{\text{src}}, \mathcal{D}_{\text{trg}}) \\ &= \arg\min_{\theta}[\mathcal{L}_{\text{SAS}} + \mathcal{L}_{\text{SA}}].\end{aligned}$$

C.2 Technical Details about Baseline Algorithms

In this section, we introduce the baselines in detail and the implementation follows the ODRL benchmark (Lyu et al., 2024b).

BOSA (Liu et al., 2024). BOSA shows a distribution shift issue might exist when learning policies from the two domain offline data under dynamics mismatch. It handles the out-of-distribution (OOD) state actions pair through a supported policy optimization and addresses the OOD dynamics issue through a supported value optimization by data filtering. Specifically, the policy is updated with:

$$\mathcal{L}_{\text{actor}} = \mathbb{E}_{s\sim\mathcal{D}_{\text{src}}\cup\mathcal{D}_{\text{trg}},\, a\sim\pi_\phi(s)}\left[Q(s, a)\right], \quad \text{s.t.} \quad \mathbb{E}_{s\sim\mathcal{D}_{\text{src}}\cup\mathcal{D}_{\text{trg}}}\left[\hat{\pi}_{\theta_{\text{offline}}}(\pi_\theta(s) \mid s)\right] > \epsilon.$$

Here, the ϵ is the threshold, $\hat{\pi}_{\theta_{\text{offline}}}$ is the learned policy for the combined offline dataset. The value function is updated with:

$$\mathcal{L}_{\text{critic}} = \mathbb{E}_{(s,a)\sim\mathcal{D}_{\text{src}}}\left[Q(s,a)\right] + \mathbb{E}_{(s,a,r,s')\sim\mathcal{D}_{\text{src}}\cup\mathcal{D}_{\text{trg}},\, a'\sim\pi_\phi(\cdot|s)}\left[I\left(\hat{p}_{\text{trg}}(s'|s,a) > \epsilon'\right)\left(Q_{\theta_i}(s,a) - y\right)^2\right],$$

where $I(\cdot)$ is the indicator function, $\hat{p}_{\text{trg}}(s'|s,a) = \arg\max E_{(s,a,s')\sim D_{\text{trg}}}[\log \hat{p}_{\text{trg}}(s'|s,a)]$ is the estimated target domain dynamics, ϵ' is the threshold.

IQL (Kostrikov et al., 2021a). IQL learns the state value function and state-action value function simultaneously by expectile regression:

$$\mathcal{L}_V = \mathbb{E}_{(s,a)\sim\mathcal{D}_{\text{src}}\cup\mathcal{D}_{\text{trg}}}\left[L_2^\tau(Q_\theta(s,a) - V_\psi(s))\right]$$

where $L_2^\tau(u) = |\tau - I(u < 0)||u|^2$, $I(\cdot)$ is the indicator function, and θ is the target network parameter. The state-action value function is then updated by:

$$\mathcal{L}_Q = \mathbb{E}_{(s,a,r,s')\sim\mathcal{D}_{\text{src}}\cup\mathcal{D}_{\text{trg}}}\left[\left(r(s,a) + \gamma V_\psi(s') - Q_\theta(s,a)\right)^2\right].$$

The advantage function is $A(s,a) = Q(s,a) - V(s)$. The policy is optimized by the advantage-weighted behavior cloning:

$$\mathcal{L}_{\text{actor}} = \mathbb{E}_{(s,a)\sim\mathcal{D}_{\text{src}}\cup\mathcal{D}_{\text{trg}}}\left[\exp(\beta\cdot A(s,a))\log\pi_\phi(a|s)\right],$$

where β is the inverse temperature coefficient.

TD3-BC (Fujimoto & Gu, 2021). TD3-BC is an effective model-free offline RL approach that incorporates a behavior cloning regularization term to the objective function of the vanilla TD3, which gives:

$$\mathcal{L}_{\text{actor}} = \lambda\cdot\mathbb{E}_{s\sim\mathcal{D}_{\text{src}}\cup\mathcal{D}_{\text{trg}}}\left[Q(s,\pi_\theta(s))\right] + \mathbb{E}_{(s,a)\sim\mathcal{D}_{\text{src}}\cup\mathcal{D}_{\text{trg}}}\left[(a-\pi_\theta(s))^2\right],$$

where

$$\lambda = \frac{\nu}{\frac{1}{N}\sum_{(s_j,a_j)} Q(s_j,a_j)} \quad \text{and} \quad \nu\in\mathbb{R}^+$$

is the normalization coefficient.

MOPO (Yu et al., 2020). MOPO is a standard model-based offline policy optimization method, which learns dynamics first and penalizes rewards by the uncertainty of the dynamics. Lastly, it optimizes a policy with the SAC (Haarnoja et al., 2018). Specifically, following previous off-dynamics work (Eysenbach et al., 2020) in the online setting that applies MBPO as a baseline, we learn the dynamics with the combined offline source and target data. We follow the implementation in OfflineRL-kit.

DARA (Liu et al., 2022). We refer to the Appendix C.1 for the details. We follow the implementation in ODRL (Lyu et al., 2024b).

C.3 Additional Experimental Results

In this section, we present additional results on various types of dynamic shifts, including Kinematic shift (kin) and Morphology shift (morph), on Mujoco and Adroit, following the ODRL benchmark. We present the results in Table 4 and Table 5, which are the detailed results of the Figure 3. We observe that our method outperforms the baseline methods in most cases, indicating that it is applicable to various types of dynamic shifts and environments.

Figure 4 summarizes the normalized scores across all environments under different shift levels on MuJoco gravity and friction shift settings. In Figure 4a, MOBODY consistently outperforms baselines under gravity shifts, with especially large gains at the more challenging and larger shift levels on 0.1 and 5.0, as MOBODY can explore more of the environment with the learned dynamics. A similar trend is observed in Figure 4b, where MOBODY again outperforms all baselines, with greater improvements in the larger shift (0.1 and 5.0) compared to the smaller ones (0.5 and 2.0).

Table 4: Performance comparison on HalfCheetah, Ant, Walker2d, and Hopper environments with kinematic and morphology shift. Our method performs best in 26 out of 32 total tasks and receives an overall 25% improvement over baselines. We use **M** and **H** to represent the medium and hard levels of the dynamics shift.

Env	Type	Level	BOSA	IQL	TD3-BC	DARA	MOPO	MOBODY
HalfCheetah	morph-thigh	M	22.83 ± 0.03	20.49 ± 0.50	19.49 ± 0.50	10.90 ± 0.43	17.32 ± 1.80	**27.18 ± 6.80**
		H	20.77 ± 0.66	21.69 ± 0.58	22.19 ± 1.08	10.35 ± 2.10	25.33 ± 2.23	**28.51 ± 9.20**
	morph-torso	M	1.67 ± 0.87	1.87 ± 0.80	5.86 ± 0.21	2.91 ± 0.08	10.65 ± 4.86	**23.92 ± 12.24**
		H	17.09 ± 15.71	27.81 ± 3.14	2.73 ± 1.25	29.41 ± 7.88	32.78 ± 4.19	**40.45 ± 1.26**
	kin-footjnt	M	**36.79 ± 0.92**	34.71 ± 0.72	30.19 ± 3.73	33.48 ± 0.34	32.49 ± 4.02	31.88 ± 3.70
		H	14.70 ± 0.92	31.68 ± 2.35	14.05 ± 2.96	31.19 ± 4.08	**33.47 ± 5.61**	18.51 ± 7.30
	kin-thighjnt	M	14.92 ± 0.01	41.27 ± 3.16	41.77 ± 2.66	15.47 ± 0.62	38.33 ± 8.68	**59.17 ± 0.85**
		H	31.72 ± 0.17	31.60 ± 9.36	31.10 ± 9.86	31.46 ± 2.31	30.35 ± 2.93	**56.72 ± 0.08**
Ant	morph-halflegs	M	49.94 ± 5.98	73.65 ± 2.70	46.60 ± 6.24	70.66 ± 3.36	66.32 ± 5.29	**79.25 ± 0.61**
		H	58.40 ± 3.41	57.51 ± 1.25	45.07 ± 2.82	58.46 ± 4.45	39.44 ± 8.57	**63.76 ± 3.27**
	morph-alllegs	M	72.02 ± 3.57	61.12 ± 9.73	47.18 ± 6.89	64.83 ± 4.49	49.19 ± 5.32	**75.24 ± 7.85**
		H	18.50 ± 4.33	10.44 ± 0.51	14.53 ± 3.74	4.47 ± 6.18	12.71 ± 1.66	**24.13 ± 0.10**
	kin-anklejnt	M	72.06 ± 4.63	**77.60 ± 3.35**	44.72 ± 15.96	75.43 ± 2.03	74.31 ± 1.92	74.92 ± 6.46
		H	63.78 ± 7.97	62.95 ± 7.88	66.22 ± 26.98	61.06 ± 4.92	63.28 ± 11.01	**76.97 ± 8.36**
	kin-hipjnt	M	38.52 ± 5.88	**60.97 ± 1.72**	26.85 ± 4.26	55.73 ± 1.93	48.91 ± 12.65	54.75 ± 4.58
		H	50.57 ± 4.89	59.31 ± 2.92	33.85 ± 5.59	58.47 ± 3.42	52.87 ± 2.99	**59.61 ± 3.11**
Walker	morph-torso	M	8.26 ± 4.83	12.35 ± 1.45	18.93 ± 9.36	15.79 ± 1.33	22.81 ± 13.78	**38.67 ± 2.05**
		H	1.61 ± 0.12	2.30 ± 0.58	1.54 ± 0.44	3.32 ± 1.13	9.92 ± 3.36	**11.96 ± 5.41**
	morph-leg	M	46.70 ± 8.39	41.12 ± 13.58	22.24 ± 9.95	39.71 ± 13.67	44.33 ± 6.66	**57.57 ± 2.00**
		H	14.37 ± 3.34	16.15 ± 3.70	49.07 ± 2.38	13.13 ± 1.24	19.62 ± 0.71	**49.12 ± 0.52**
	kin-footjnt	M	17.99 ± 1.15	56.62 ± 12.10	43.31 ± 20.48	55.81 ± 1.36	57.92 ± 5.95	**67.56 ± 3.05**
		H	25.76 ± 15.99	6.52 ± 1.61	26.34 ± 13.24	9.63 ± 0.91	37.21 ± 20.52	**57.93 ± 0.37**
	kin-thighjnt	M	47.63 ± 27.26	61.28 ± 14.24	35.64 ± 11.74	56.28 ± 13.79	68.11 ± 3.60	**69.48 ± 4.22**
		H	48.66 ± 14.73	51.66 ± 2.05	43.88 ± 11.54	63.76 ± 2.06	73.52 ± 7.92	**78.14 ± 2.50**
Hopper	morph-foot	M	12.67 ± 0.00	32.99 ± 0.16	12.69 ± 0.43	**40.61 ± 1.64**	12.96 ± 0.14	13.05 ± 0.48
		H	10.13 ± 0.62	11.78 ± 0.09	14.15 ± 4.30	13.32 ± 1.48	47.19 ± 12.77	**65.02 ± 11.98**
	morph-torso	M	15.88 ± 1.18	13.38 ± 0.05	13.94 ± 0.75	13.29 ± 0.19	14.04 ± 0.35	**20.23 ± 1.29**
		H	11.73 ± 0.33	7.77 ± 3.73	11.54 ± 0.81	4.15 ± 0.05	11.83 ± 0.28	**12.34 ± 0.20**
	kin-legjnt	M	36.51 ± 1.51	42.28 ± 0.08	11.76 ± 4.60	44.67 ± 0.58	43.57 ± 0.80	**54.89 ± 0.26**
		H	36.13 ± 1.70	45.02 ± 4.08	18.87 ± 1.46	**65.44 ± 4.10**	50.38 ± 3.74	56.88 ± 3.68
	kin-footjnt	M	14.92 ± 0.01	15.58 ± 0.11	17.09 ± 0.04	15.47 ± 0.62	31.33 ± 16.25	**33.94 ± 14.81**
		H	31.72 ± 0.17	32.41 ± 0.16	32.21 ± 0.00	32.99 ± 0.78	33.21 ± 0.07	**33.35 ± 0.89**
Total			964.95	1123.88	865.60	1101.65	1205.70	**1515.10**

Table 5: Performance comparison on Pen and Door tasks. Our method performs the best compared with the baselines and receives an overall 10% improvement. We use **M** and **H** to represent the medium and hard levels of the dynamics shift.

Env	Type	Level	BOSA	IQL	TD3-BC	DARA	MOPO	MOBODY
Pen	kin-broken-jnt	M	30.63 ± 9.01	24.34 ± 15.49	6.86 ± 6.63	**38.60 ± 3.44**	37.99 ± 7.46	37.67 ± 4.54
		H	7.18 ± 2.02	7.74 ± 3.48	1.31 ± 1.29	9.41 ± 6.06	8.14 ± 2.92	**13.73 ± 6.32**
	morph-shrink-finger	M	10.72 ± 6.65	13.75 ± 4.91	2.20 ± 1.71	8.72 ± 3.12	3.48 ± 0.85	**16.48 ± 10.46**
		H	11.78 ± 6.57	32.16 ± 1.14	9.12 ± 9.03	22.17 ± 3.90	28.89 ± 2.48	**37.80 ± 1.18**
Door	kin-broken-joint	M	25.42 ± 22.04	37.43 ± 12.76	-0.23 ± 0.01	20.18 ± 5.29	27.90 ± 7.92	**39.26 ± 3.72**
		H	30.64 ± 26.87	56.02 ± 7.74	-0.12 ± 0.02	58.22 ± 9.91	57.45 ± 9.58	**61.61 ± 9.84**
	morph-shrink-finger	M	41.59 ± 5.95	60.74 ± 12.83	-0.19 ± 0.01	50.32 ± 4.78	52.02 ± 1.74	**63.67 ± 9.52**
		H	26.97 ± 8.62	**68.64 ± 8.34**	-0.20 ± 0.02	44.22 ± 7.19	67.06 ± 1.96	62.88 ± 5.25
Total			184.93	300.82	18.75	251.84	282.93	**333.10**

Existing methods, DARA and BOSA, fail in large shift settings as the reward regularization methods cannot account for the large shift, as they are mainly trained with source data with regularization, thus usually receive high rewards in the source domain, but don't really adapt to the target domain, especially in large shifts, as the policy gets different rewards. Also, they lack the exploration of the target domain.

C.4 Additional Ablation Study Results

In this section, we present additional ablation studies results on Hopper as we mentioned in Section 4.3. Same as Table 2, we evaluate the overall effectiveness of each component (A1 and A2) and then analyze specific design choices (A3 and A4). For dynamics learning, we assess the impact of the cycle transition loss and representation learning. For policy learning, we examine the effectiveness of the Q-weighted loss. We draw the same conclusion as Section 4.3.

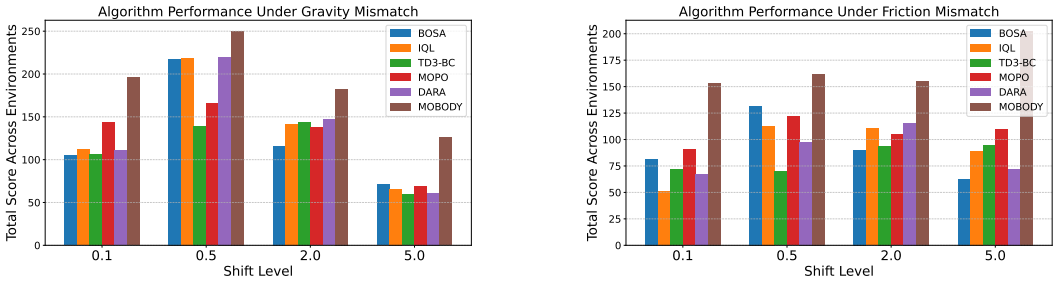

(a) Gravity Shift

(b) Friction Shift

Figure 4: Performance of our MOBODY and baselines in different dynamics shift with various shift levels $\{0.1, 0.5, 2.0, 5.0\}$. The scores are summed over all the environments (HalfCheetah, Ant, Walker2D, and Hopper) in the target domain. We directly compare the algorithms in the same dynamics shift levels. The higher scores indicate better performance. We can observe a larger improvement for larger shift cases (0.1 and 5.0).

Table 6: Performance of ablation study of our proposed MOBODY method. The experiments are conducted on the Hopper environments under the medium-level with dynamics shifts in gravity and friction in $\{0.1, 0.5, 2.0, 5.0\}$ shift levels. The source domains are the original environments and the target domains are the environments with dynamics shifts. We report the normalized scores in the target domain with the mean and standard deviation across three random seeds. The higher scores indicate better performance.

Env	Level	Algorithm Ablation		Loss Ablation		MOBODY
		A1	A2	A3	A4	
Hopper Gravity	0.1	14.53 ± 2.81	28.07 ± 4.12	33.65 ± 3.21	11.54 ± 1.12	36.25 ± 1.50
	0.5	28.83 ± 3.32	25.70 ± 1.86	23.52 ± 3.33	20.11 ± 1.26	33.57 ± 6.71
	2.0	10.64 ± 1.92	12.32 ± 5.21	10.90 ± 1.29	16.40 ± 4.12	23.79 ± 2.09
	5.0	8.12 ± 0.69	8.23 ± 1.92	8.79 ± 0.94	8.89 ± 1.01	8.06 ± 0.03
Hopper Friction	0.1	26.09 ± 4.75	35.14 ± 7.97	24.42 ± 2.86	20.07 ± 10.32	51.19 ± 2.56
	0.5	22.42 ± 3.32	31.31 ± 5.08	29.26 ± 6.02	27.07 ± 3.73	41.34 ± 0.49
	2.0	10.64 ± 0.32	9.41 ± 1.03	10.31 ± 0.12	8.47 ± 1.13	11.00 ± 0.14
	5.0	8.43 ± 1.32	7.52 ± 0.29	8.14 ± 0.91	7.55 ± 1.02	8.07 ± 0.04

Hyperparameter Analysis. We conducted two hyperparameter analyses: the BC loss weight and uncertainty penalty of the model-based method in the policy learning part, as detailed in Table 7. We can see that these parameters are important in the performance of BC loss and need to be tuned across different tasks and environments. It is interesting to note that even the suboptimal parameters (0.05) in Table 7 outperform the baseline algorithms.

Rule of thumb hyperparameters. We notice that there is no universal set of hyperparameters that works well across all tasks with different environments, shift types, and levels. Even without the dynamics shift, model-based RL methods typically require different hyperparameters for different environments. But empirically, we could have a set of hyperparameters that generally receives a relatively good performance for most tasks, i.e., weight of BC = 0.1 and MOPO penalty = 5. From there, we primarily tune the BC loss weight based on the convergence behavior of the policy. In most cases, using a MOPO penalty of 5 and a BC loss weight selected from the range 0.05, 0.1, 1, 2 yields strong performance. Overall, the number of hyperparameters is modest compared to those commonly required in offline model-based RL methods.

Computational Resources We run all experiments on a single GPU (NVIDIA RTX A5000, 24,564 MiB) paired with 8 CPUs (AMD Ryzen Threadripper 3960X, 24-Core). Each experiment requires approximately 12 GB of RAM and 20 GB of available disk space for data storage.

Computational Cost We provide an estimated running time of MOPO, DARA, BOSA and our method in Appendix C.4. The running time of MOBODY requires approximately 25% more time to

Table 7: Hyperparameters of the policy learning. Our method is not very sensitive to the hyperparameters.

Task	BC-Weight / Uncertainty Penalty	1	5	10
Walker2d-Friction-0.5	0.05	76.96 ± 1.99	55.67 ± 21.18	51.43 ± 19.37
	0.1	75.64 ± 11.05	70.49 ± 2.81	62.54 ± 5.49
	1	75.63 ± 2.57	82.91 ± 4.43	62.50 ± 6.83
Walker2d-kin-footjnt-medium	0.05	67.56±3.05	56.88±1.47	65.14±2.57
	0.1	62.19±5.27	64.17±3.62	66.30±0.01
	1	59.33±5.15	62.69±5.00	62.56±1.09
Walker2d-kin-footjnt-hard	0.05	40.96±1.58	57.75±0.34	57.59±0.47
	0.1	57.93±0.37	56.27±1.12	43.13±15.51
	1	34.31±21.12	53.92±3.74	43.74±14.06
Walker2d-kin-thighjnt-medium	0.05	69.48±4.22	60.40±4.27	66.85±6.90
	0.1	65.13±3.72	65.24±2.10	64.19±1.22
	1	64.17±1.83	62.10±5.88	70.39±0.28
Walker2d-kin-thighjnt-hard	0.05	78.14±2.50	59.21±4.79	70.20±2.71
	0.1	76.50±1.49	61.96±6.71	55.95±16.29
	1	69.45±1.78	66.92±0.04	71.38±5.42

run 1 million steps compared to model-free DARA and is faster than the BOSA. The extra running time is due to the dynamic learning and generation of rollouts. On the other hand, MOPO and MOBODY have similar running times. This demonstrates that we have a similar computational cost and running time compared to the existing model-based method, as the additional loss calculation doesn't significantly increase the computation time.

Table 8: Running time comparison on A5000, AMD Ryzen Threadripper 3960X 24-Core Processor. .

	Walker2d-Gravity-0.5	HalfCheetah-Gravity-0.5
BOSA	∼3 hours	∼3.5 hours
DARA	∼2 hours	∼2.5 hours
MOPO	∼2.5 hours	∼3 hours
MOBODY	∼2.5 hours	∼3 hours

C.5 Environment Setting

Gravity Shift. Following the ODRL benchmark (Lyu et al., 2024b), we modify the gravity of the environment by editing the gravity attribute. For example, the gravity of the HalfCheetah in the target is modified to 0.5 times the gravity in the source domain with the following code.

```
# gravity
<option gravity="0 0 -4.905" timestep="0.01"/>
```

Friction Shift The friction shift is generated by modifying the friction attribute in the geom elements. The frictional components are adjusted to $\{0.1, 0.5, 2.0, 5.0\}$ times the frictional components in the source domain, respectively.

Kinematic Shift The kinematics shift is simulated through broken joints by limiting the rotation ranges of some hand joints. We consider the broken ankle joint, hip joint, foot joint, etc, for Mujoco and Adroit environments.

Morphology Shift The morphology shift is achieved by modifying the size of specific limbs or torsos of the simulated robot in Mujoco and shrink the finger size in the manipulation task, without altering the state space and action space.

D LIMITATION

MOBODY relies on the assumption that the source and target domains share a common state representation ϕ_E and transition ϕ_T that map the unified latent state action representation to the next state. In future work, we plan to explore how to effectively learn a dynamics model for the target domain when this assumption does not hold.

USAGE OF LLM

All ideas and research are conducted by the author, and the paper itself is written by the author. The LLM is used as a tool for polishing the written content of the paper and checking the grammar erorrs.

Table 9: Hyperparameter of the MOBODY and baselines.

Hyperparameter	Value
Shared	
Actor network	(256, 256)
Critic network	(256, 256)
Learning rate	3×10^{-4}
Optimizer	Adam
Discount factor	0.99
Replay buffer size	10^6
Nonlinearity	ReLU
Target update rate	5×10^{-3}
Source domain Batch size	128
Target domain Batch size	128
MOBODY	
Latent dimensions	16
State encoder	(256, 256)
State action encoder	(32)
Transition	(256, 256)
Representation penalty λ_{rep}	1
Rollout length	1, 2 or 3
MOPO-Style Reward Penalty β	1,5 or 10
Q-weighted behavior cloning	0.05, 0.1 or 1
Classifier Network	(256, 256)
Reward penalty coefficient λ	0.1
DARA	
Temperature coefficient	0.2
Maximum log std	2
Minimum log std	-20
Classifier Network	(256, 256)
Reward penalty coefficient λ	0.1
BOSA	
Temperature coefficient	0.2
Maximum log std	2
Minimum log std	-20
Policy regularization coefficient λ_{policy}	0.1
Transition coefficient $\lambda_{\text{transition}}$	0.1
Threshold parameter ϵ, ϵ'	$\log(0.01)$
Value weight ω	0.1
CVAE ensemble size	1 for the behavior policy, 5 for the dynamics model
IQL	
Temperature coefficient	0.2
Maximum log std	2
Minimum log std	-20
Inverse temperature parameter β	3.0
Expectile parameter τ	0.7
TD3_BC	
Normalization coefficient ν	2.5
BC regularization loss	0.05, 0.1 or 1
MOPO	
Transition	(256,256,256)
Maximum log std	2
Minimum log std	-20
Reward penalty τ	1, 5 or 10
Rollout Length	1, 2 or 3